**Smart Structures and Systems**, *Vol. 25, No. 6 (2020) 765-778*
DOI: https://doi.org/10.12989/sss.2020.25.6.765


# Hybridized dragonfly, whale and ant lion algorithms in enlarged pile's behavior

Xinyu Ye [1], Zongjie Lyu [2] and Loke Kok Foong [*3,4]

[1] *School of Civil Engineering, Central South University, Changsha 410075, China*
[2] *Institute of Research and Development, Duy Tan University, Da Nang 550000, Vietnam*
[3] *Department for Management of Science and Technology Development, Ton Duc Thang University, Ho Chi Minh City, Vietnam*
[4] *Faculty of Civil Engineering, Ton Duc Thang University, Ho Chi Minh City, Vietnam*

(*Received November 28, 2019, Revised February 10, 2020, Accepted February 14, 2020*)

**Abstract.** The present study intends to find a proper solution for the estimation of the physical behaviors of enlarged piles through a combination of small-scale laboratory tests and a hybrid computational predictive intelligence process. In the first step, experimental program is completed considering various critical influential factors. The results of the best multilayer perceptron (MLP)-based predictive network was implemented through three mathematical-based solutions of dragonfly algorithm (DA), whale optimization algorithm (WOA), and ant lion optimization (ALO). Three proposed models, after convergence analysis, suggested excellent performance. These analyses varied based on neurons number (e.g., in the basis MLP hidden layer) and of course, the level of its complexity. The training $R^2$ results of the best hybrid structure of DA-MLP, WOA-MLP, and ALO-MLP were 0.996, 0.996, and 0.998 where the testing $R^2$ was 0.995, 0.985, and 0.998, respectively. Similarly, the training RMSE of 0.046, 0.051, and 0.034 were obtained for the training and testing datasets of DA-MLP, WOA-MLP, and ALO-MLP techniques, while the testing RMSE of 0.088, 0.053, and 0.053, respectively. This obtained result demonstrates the excellent prediction from the optimized structure of the proposed models if only population sensitivity analysis performs. Indeed, the ALO-MLP was slightly better than WOA-MLP and DA-MLP methods.

**Keywords:** smart structures; enlarged piles; WOA-MLP; DA-MLP; ALO-MLP; multilayer perceptron

## 1. Introduction

Enlarged piles built from common concrete and have been employed to increase the ultimate axial pullout the capacity of constructed shafts. Besides, the geometry of the base is known to be a vital issue. The enlarged piles generally include one or more of inverted cones (Bui *et al*. 2019b). Consequently, various mathematical solutions have been employed to calculate the pile behavior reliably (Ghiasi and Ghasemi 2018, Li *et al*. 2018, Bozorgvar and Zahrai 2019, Duan *et al*. 2019). These techniques have been used to estimate the (i) pile dynamic capacity; (ii) pile settlements; (iii) uplift capacity of suction caisson; (iv) bearing capacity of pile foundation; (v) pile setup, or foundation vibrations. Notably, scholars proposed diverse approaches for estimating the engineering complex problems heating and cooling loads of residential buildings (Zhou *et al*. 2020a), energy storage (Tien Bui *et al*. 2019), rock mechanics as well as employed predictive techniques such as wavelet transform-based hybrid model (Qiao and Yang 2019), machine learning in general (Yuan and Moayedi 2019), particle swarm optimization (Wang *et al*. 2019), quantum dolphin swarm algorithm, improved lion swarm optimizer, whale optimization algorithm, modified dolphin swarm algorithm, Harris hawks' optimization, improved dolphin swarm algorithm, but they are not reliable enough to provide such an excellent output avoiding uncertainty in estimating the pile uplift capacity (Guo *et al*. 2020, Mehrabi *et al*. 2020). Also, there is not a proper analysis according to an extensive number of experimental laboratory schedule (Bui *et al*. 2019a, Nguyen *et al*. 2019, Xi *et al*. 2019). Shi *et al*. (1998) have described in situ experiments on bearing capacity of enlarged piles, along with the verifying of the significant parameters influencing the deformation and load behaviors of enlarged piles. Some of these critical parameters include hydro-geologic case, primary size of piles, and installing method, and resulting from that the enlarged piles in length. Chae *et al*. (2012), applied proper use of field data monitoring, have studied the uplift force of enlarged pile placed in UAE, Persian Gulf. The experiments consist of several real-scale uplift loading experiments located in Abu Dhabi. The comparison of theoretical models and 3D finite element (FE) results, shows the 3D analysis has overestimated the final uplift forces of the enlarged based pile even though the bell-shaped was not taken into consideration (Chae *et al*. 2012). An elastic-plastic advanced computational-based solution for the uplift of the enlarged pile has been conducted by Yao and Chen (2014). Finding a reliable mathematical solution for complex problems is known as a difficult task for civil engineers. There have been numerous engineering examples of the laboratory and field simulation (Zhang *et al*. 2018, Saleem and Jo 2019). One of the well-

∗Corresponding author, Ph.D.,
E-mail: lokekokfoong@tdtu.edu.vn
[a] Ph.D., E-mail: yexinyu113@csu.edu.cn
[b] M.Sc., E-mail: zongjielyu@duytan.edu.vn


http://www.techno-press.org/?journal=sss&subpage=7
ISSN: 1738-1584 (Print), 1738-1991 (Online)

established methods in training the databases (e.g., making links between basic inputs and outputs of the problems) is highlighted based on the connections among human neurons, and it is scientifically called artificial neural network (ANN) (Zhou *et al*. 2020b). The idea of ANN is firstly mentioned by McCulloch and Pitts (1943) and processed by many researchers. Though, the first researcher who proposed this technique to be suggested to training an issue was Hebb (1949). Some rules are existing in the case of ANN which is mainly according to direct observations and also the neuro-physiologic nature hypothesis. The multilayer perceptron (i.e., one type of ANN learning technique) model can result predictive network (according to the database utilize for training). The proposed networks enable having an estimation of the values to an unavailable result. It is important to know that the major concern in these investigations is how identically they may estimate the unknown results (we can consider it as a target that requries to be obtained using the trained network).

Hybrid soft computing techniques have been successfully employed in various applications and research projects. Different examples of soft computing are utilized for soil compression coefficient In recent years, many new hybrid computational algorithms are developed such as, genetic Programming (GP), chaotic moth-flame optimization (Wang *et al*. 2017), bacterial foraging optimization (Xu and Chen 2014, Chen *et al*. 2020), improved ant colony optimization (Zhao *et al*. 2014), fruit fly optimization (Shen *et al*. 2016), grey wolf optimization (Zhao *et al*. 2019), Moth-flame optimizer (Xu *et al*. 2019), multi-swarm whale optimizer (Wang and Chen 2020), etc. have become popular among the researchers because they can provide estimations with optimal accuracy when modeling complicated phenomena. Ardalan *et al*. (2009) have combined a technique called Group Method of Data Handling (GMDH) with Genetic Algorithms (GA) to predict the values of pile shaft friction. Moreover, Alavi *et al*. (2011) have applied three genetic programming based techniques, linear-genetic programming (LGP), the tree formed genetic programming (TGP), and gene expression programming (GEP) to provide the reliable mathematical formula of the pullout capacity. The proposed equations could predict pullout forces in suction caissons. In a separate study, Cheng *et al*. (2014) have employed radial basis function (RBF) IFRIM techniques (as abbreviated from neural network hybrid inference model), as well as artificial bee colony (ABC), and fuzzy logic (FL) to predict the suction caissons' uplift capacity. Wu *et al*. (2015) have generated an analysis technique in an axially loaded single bored pile. They employed a nonlinear soft technique resulting that the side friction's soft features could be predicted with reasonable accuracy. Thomas *et al*. (2016) have established a novel model as an Adaptive neuro-fuzzy inference system (ANFIS) to estimate the parameters associated with ground motion as well as seismic signals.

In this regard, recently, hybrid computational intelligence is getting much attentions to predict the pullout bearing capacity pile foundations. However, providing a reliable large-scale experimental program has always been struggling. Preparation of such a database, including the outputs of centrifuge tests, requires excellent knowledge of data collection through a vast number of experiments. The main objective of the present research is to simulate the physical behaviors of under reamed piles through laboratory and hybrid computational intelligence techniques. In this regard, two artificial intelligent techniques-based solutions were utilized. For checking the reliability of the method (for example, the comparison among the exact target and the output of this network) calculation procedure of the network error is selected according to the comparison among the predicted results and the measured values taken from the laboratory or other real experiments. To calculate the network validity on estimating the outputs, various statistical indices may be suggested, like root mean squared error (RMSE) and coefficient of determination ($R^2$). First of all, artificial intelligent techniques were utilized. To find the best network structure, a total of 48 dissimilar MLP simulations and required number of evolutionary hybrid elephant herding optimization (DA), whale optimization algorithm (WOA), an ant lion optimization (ALO) for the calculation of pullout capacity ($P_{ult}$) are performed.

## 2. Methodology and established database

The database that is used for proposing a new learning system in this research included a total of 36 small-scale pullout capacity experiments on enlarged piles (Nazir *et al*.

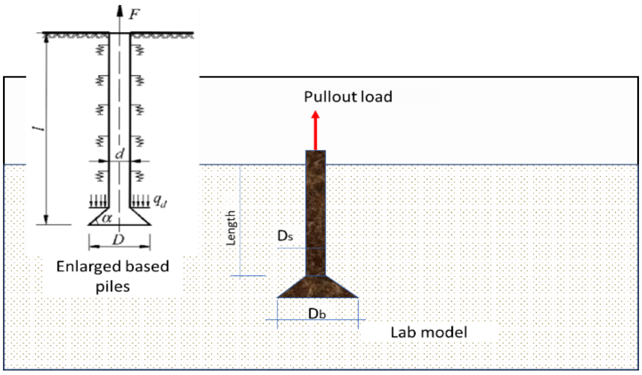


Fig. 1 A sample of the enlarged base pile and critical parameters for modeling

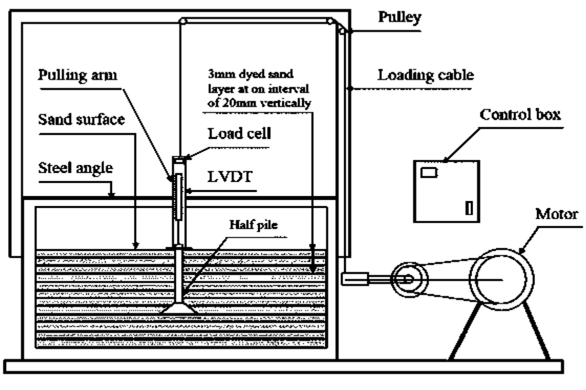


Fig. 2 Small-scale laboratory pullout capacity tests on enlarged piles (Nazir *et al*. 2015)

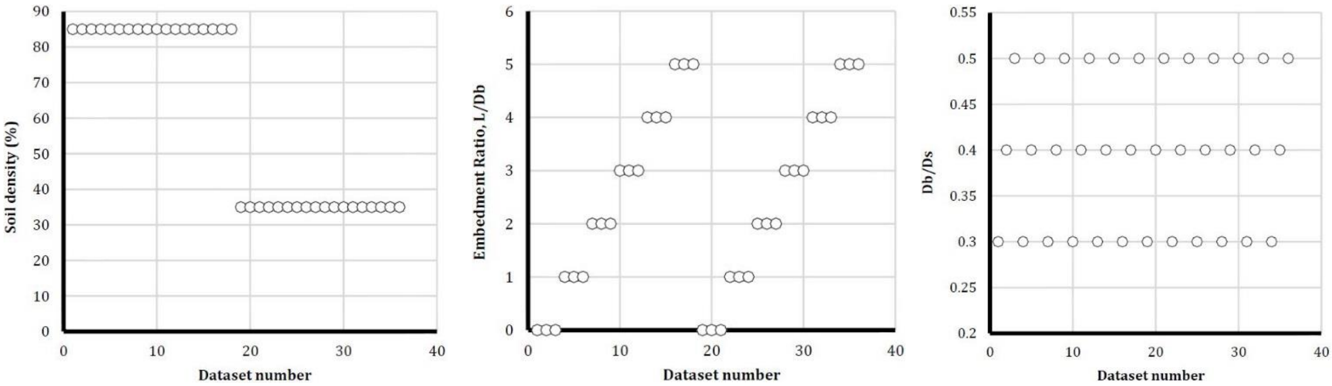


(a) Soil density (b) Embedment ratio ($L/D_b$) (c) $D_b/D_s$

Fig. 3 Graphical qualification of the range of input information versus data numbers

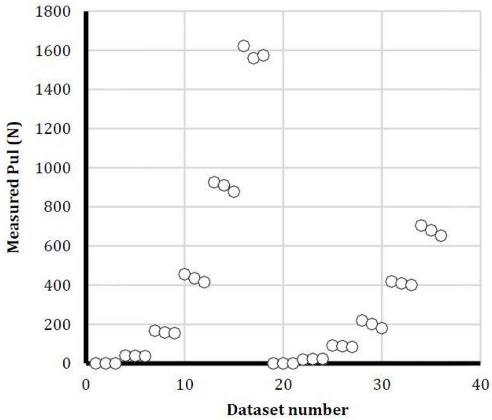


Fig. 4 $P_{ult}$ Output information versus data numbers

2015). The tests were performed on a small-scale pile model with an enlarged (i.e., type of pile that the base diameter is intentionally considered higher than the shaft diameter) base, a pile diameter of $D_s$ varied from 30 mm to 50 mm, a base diameter of $D_b$ = 75, 100, 125 and 150 mm, and finally a base angle of α = 30°, 45°, and 60°. The tests were done in both loose and dense sand density conditions. As one more criterion influencing the outputs of the study, the enlarged piles were installed considering several embedment ratios, $L/D_b$ ranging between 1 and 5. The details of a sample of the enlarged pile and small-scale through the experimental program are shown in Figs. 1 and 2, respectively. A suitable prediction procedure, which is employed by neural network-based simulation models, need to be settled by two main steps such as (i) initial normalization to the values of -1.0 to + 1.0 (called also data pre-processing) and later on data processing, (ii) selecting a properly structures hybrid algorithm. The dataset showed here was then normalized. The normalization consists of all three main inputs, affecting the ultimate pullout bearing capacity ($P_{ult}$) of the enlarged piles and output layer.

The key input parameters implemented in the analysis comprises of soil density value ($D_r$), under reamed embedment length ratio ($L/D_b$), and the ratio of base diameter to shaft diameter ($D_b/D_s$), where the output was taken pullout bearing capacity of the $P_{ult}$. The predicted results for both datasets from the ANN model was evaluated based on several statistical indices. Also, to assess the reliability of proposed networks, two ranking methods of (i) color intensity, and (ii) total ranking method (TRM) were used. Note that these ranking systems were used according to the result of their commendable statistical indices. The graphical qualification of the range of input information against data numbers for employed input layers is shown in Fig. 3. The variation of the main output is shown in Fig. 4. Besides, the histogram distribution of the input data layers and $P_{ul}$ output layer is illustrated in Figs. 5 and 6, respectively. Table 1 shown statistical analysis of $P_{ult}$ based on three features after the Kolmogorov-Smirnov test.

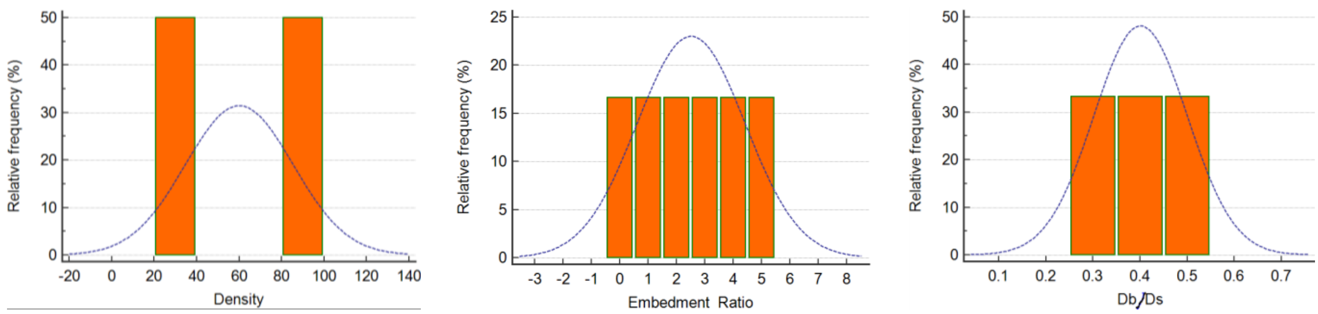


(a) Soil density (b) Embedment ratio ($L/D_b$) (c) $D_b/D_s$

Fig. 5 Histogram of the input data layers, (a) soil density; (b) ($L/D_b$); (c) $D_b/D_s$

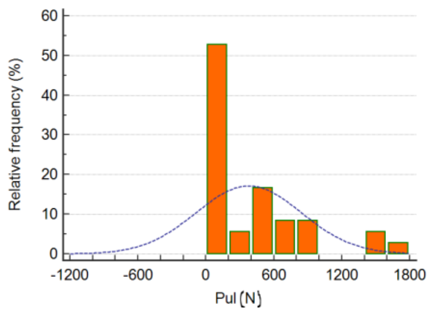


Fig. 6 Histogram of the $P_{ult}$ Output as the main output

### *2.1 Methodology*

**Multilayer-perceptron:** Among the most effective tools that have been used in the last two decades are artificial neural networks (ANNs), which were first introduced by McCulloch and Pitts (1943). These tools are widely applied for modeling complex engineering issues. ANN theory is inspired by a biological neural network (Jain *et al*. 1996), where the models can learn through establishing non-linear equations between the input and output dataset (Rao 2000). A typical ANN architecture is composed of some layers that contain components called neurons (i.e., shown in Fig. 7). In a neural learning approach, a significant role is done using computation neurons. A common type of ANN is the multi-layer perceptron (MLP), which is distinguished by three sorts of the layer. The input layer receives the input data, and the number of neurons in it equals the number of input parameters. After that, there can be one or more hidden layer(s) containing computation neurons and, finally, we have one output layer. Similar to the input layer, the number of neurons in the last layer equals the number of output parameters. As was explained, a specific architecture can have more than one hidden layer, but theoretical works have shown that a single hidden layer can present a good approximation for any complex problem (Hornik *et al*. 1989, Soleimani *et al*. 2018). More specifically, for each neuron, if we assume X as the input and W as the interconnected weight, the bias term of β will be added to the summation of WXs. In the following, an activation

Table 1 Statistical analysis of $P_{ult}$ based on three features after the Kolmogorov-Smirnov test

| | **Embedment ratio** | **Db/Ds** | **LAB - Pul** |
|---|---|---|---|
| Sample size | 36 | 36 | 36 |
| Lowest value | 0 | 0.3 | 0 |
| Highest value | 5 | 0.5 | 1622.47 |
| Arithmetic mean | 2.5 | 0.4 | 376.8667 |
| 95% CI for the Arithmetic mean | 1.9140 to 3.0860 | 0.3720 to 0.4280 | 219.5001 to 534.2333 |
| Median | 2.5 | 0.4 | 173.66 |
| 95% CI for the median | 1.6589 to 3.3411 | 0.3659 to 0.4341 | 69.3729 to 416.4290 |
| Variance | 3 | 0.006857 | 216316.3346 |
| Standard deviation | 1.7321 | 0.08281 | 465.0982 |
| Relative standard deviation | 0.6928 (69.28%) | 0.2070 (20.70%) | 1.2341 (123.41%) |
| Standard error of the mean | 0.2887 | 0.0138 | 77.5164 |
| Coefficient of Skewness | 0.0000 (P = 1.0000) | -3.3041E-015 (P = 1.0000) | 1.5461 (P = 0.0007) |
| Coefficient of Kurtosis | -1.2770 (P = 0.0024) | -1.5441 (P < 0.0001) | 1.7420 (P = 0.0641) |
| Kolmogorov-Smirnov testa | D = 0.1401 | D = 0.2197 | D = 0.2162 |
| For normal distribution | Accept normality (P = 0.0716) | Reject normality (P = 0.0001) | Reject normality (P = 0.0002) |

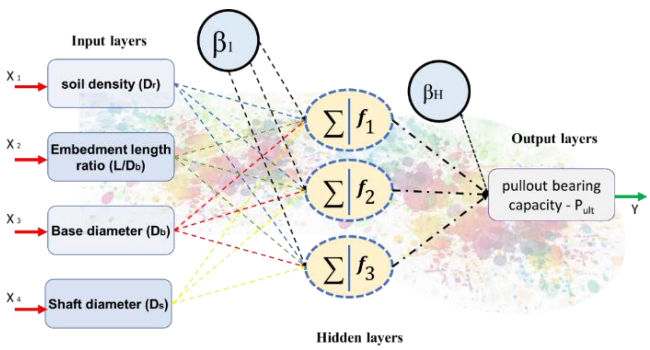


(a)

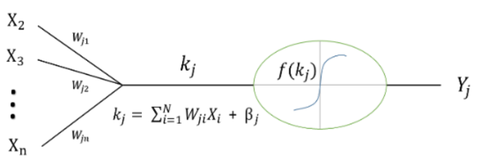


(b)

Fig. 7 Typical structure and operation of MLP function ($f$(I)) will be applied to the acquired term ($\sum$ WX + β) to produce the outputs. The activation function for this case was considered as Tan-sigmoid (Tansig), which is defined by Eq. (1)

$$Tansig(x) = \frac{2}{1+e^{-2x}} - 1 \tag{1}$$

In addition to training the network, the Levenberg–Marquardt technique (trainLM) was selected because it provides proper performance compared to the conventional gradient descent methods (Hagan and Menhaj 1994, El-Bakry 2003). Also, the backpropagation method was applied to adjust the calculated weights and biases in each iteration to achieve the minimum error (Hertz 2018).

This investigation aimed to predict $P_{ult}$ in buildings utilizing artificial intelligence according to predictive tools. In the case of an ANN multilayer perceptron (MLP) is employed to estimate the $P_{ult}$. The prepared datasets are parted within two sections of the training and testing model. The first section that is selected using 70% of the whole database is considered for the training the ANN models (named training dataset) while the 30 % remained items set to be used for evaluation of their network performances (called testing dataset). The new testing dataset (i.e., selected in each stage of the network simulation) is built using data that varies from the training step. Two statistical indices of determination coefficient ($R^2$) and root mean square error (RMSE) is employed to compute the network error efficiency and the regression among the target values and system outcomes of $P_{ult}$. The upper mentioned indices are significantly utilized and also are presented by the Eqs. (2) and (3), respectively.

$$RMSE = \sqrt{\frac{1}{N}\sum_{i=1}^{N}[(Y_{i_{actual}} - Y_{i_{produced}})]^2} \tag{2}$$

$$R^2 = 1 - \frac{\sum_{j=1}^{N}[(Y)_{actual,j} - (Y)_{produced,j})]^2}{\sum_{j=1}^{N}[(Y)_{actual,j} - (Y)_{mean})]^2} \tag{3}$$

where, $Y_{i\ actual}$, $Y_{i\ produced}$, and $Y_{mean}$ indicates values considered in each step of the simulation for the exact, predicted, and the mean values of showed $P_{ult}$, respectively. Besides, the factor N displays the number of datasets.

**Dragonfly Algorithm:** Proposed by Mirjalili (2016), the dragonfly algorithm (DA) mimics the dynamic and static conducts of dragonflies for optimization aims. Many scholars have successfully used the DA for non-linear engineering problems (Vanishree and Ramesh 2018, Moayedi *et al*. 2019). The cycle of dragonfly's life comprises two major stages, namely the nymph and transformation to the adult. Note that the mentioned cycle mostly relies on the first stage. The exploration could be defined in dynamic conducts where dragonflies join some groups and seek food sources (Wikelski *et al*. 2006). The Reynolds swarm intelligence is the basis of this algorithm, which follows three distinct principles: namely separation, alignment, and cohesion, to discover the solution of weights (Fig. 8)

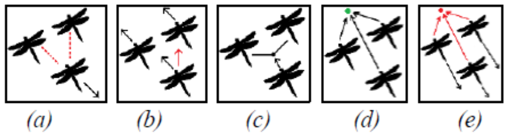


Fig. 8 Different stages of the dragonfly algorithm (DA) (after Yasen *et al*. (2018)). (a)-(e) the DA process of nymph and transformation to the adult

(a) In the separation, the dragonflies avoid other individuals because of the collision in a stationary position from the vicinity.
(b) During the alignment, the velocity of the members coordinates with each other in the vicinity.
(c) In the cohesion, the members fly toward the group midpoint in the vicinity.

Notably, the position of each swarm is updated through two natures of (i) considering prime principals for captivating the food sources, and (ii) diverting the sources out from invaders (Palappan and Thangavelu 2018).

**Whale Optimization Algorithm (WOA):** As the name implies, the WOA is inspired by the social behavior of whale herds, and more clearly, the specific nature inspired-based bubble-net hunting conduction of humpback whales. This technique is first proposed by Mirjalili and Lewis (2016). Fig. 9 displays the humpback whale's bubble-net feeding behavior. The WOA comprises three operational steps of shrinking encircling hunt, exploitation (i.e., the bubble-net attacking), and exploration (i.e., searching for the prey) (Mirjalili and Lewis 2016, Rana and Latiff 2018). In this algorithm, since there is no information about the optimal hunting place, the target prey is considered as the most appropriate candidate for the problem solution. In the exploitation phase, some spiral mathematical approaches are applied in order to detect the equidistance between the prey and whale positions. The involving whales also try to update their positions close to the most successful member. The algorithm continues improving the solution until a stopping criterion is met.

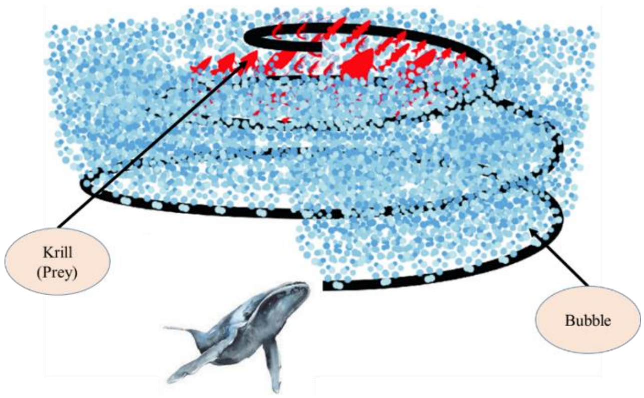


Fig. 9 The humpback whales bubble-net feeding

**Ant lion optimization:** Imitating the herding behavior of ant lions in their larvae life period, Mirjalili (2015) developed an ant lion optimization (ALO) algorithm as a new capable metaheuristic technique. In the ALO, primary locations of the target hunt and ant lions are stochastically defined in the existing search space. This algorithm comprises six steps in each repetition including (a) random walk of prey, (b) trapping in holes, (c) constructing a trap, (d) sliding of prey towards the ant lion, (e) catching the prey/reconstructing the hole, and (f) determining the elite ant lion (Mirjalili 2015).

A cumulative sum ($C_{sum}$) function is defined to express the movement of the target prey, which is mainly ant

$$X(t) = [0, Csum\left(2r(t_1)\right) - 1, \ldots, Csum\left(2r(t_n)\right) - 1] \tag{4}$$

$$r(t) = \begin{cases} 1, rand\ (0,1) > 0.5 \\ 0, rand\ (0,1) \leq 0.5 \end{cases} \tag{5}$$

Then, a normalization function (Eq. (21)) is applied at the $t^{th}$ repetition, where $d_i^t$ and $c_i^t$ symbolize the maximum and minimum of the proposed variable, $b_i$ and $a_i$ denote the maximum and minimum of random.

$$X_i^t = \frac{(X_i^t - a_i).(d_i^t - c_i^t)}{b_i - a_i} + c_i^t \tag{6}$$

where $X_i^t$ is the position of the $i^{th}$ variable.

Also, assuming $Antlion_j^t$ as the position of $j^{th}$ ant lion, and $d^t$ and $c^t$ as the maximum and minimum of all variables, the mathematical effect of the ant lion's holes on the random walk of the prey is expressed by Eqs. (22) and

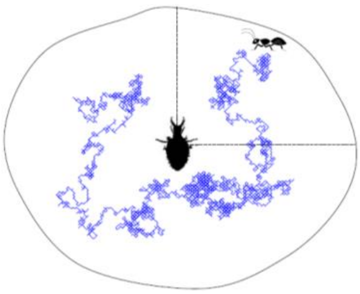

(a)

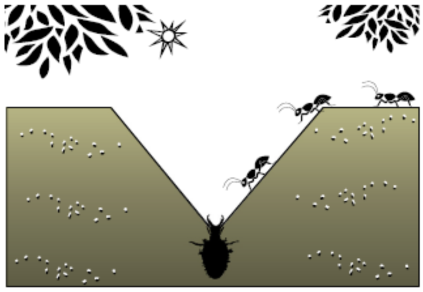

(b)

Fig. 10 (a) Random walk of the prey inside the trap; and (b) the hunting behavior of ant lions (after (Mirjalili 2015))

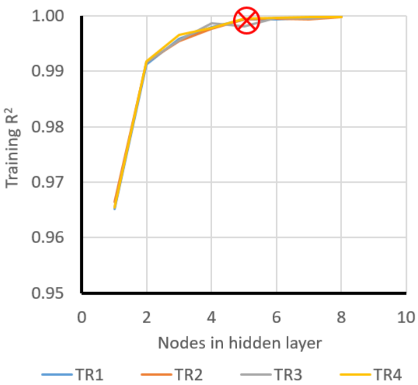


(a)

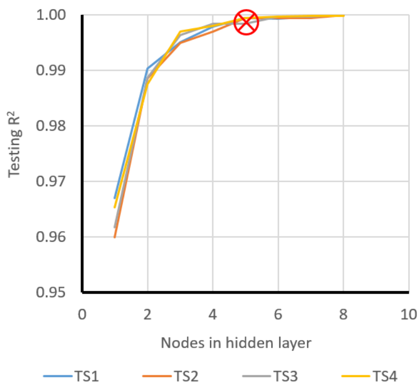


(b)

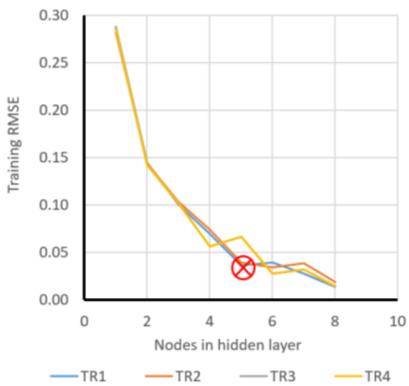


(c)

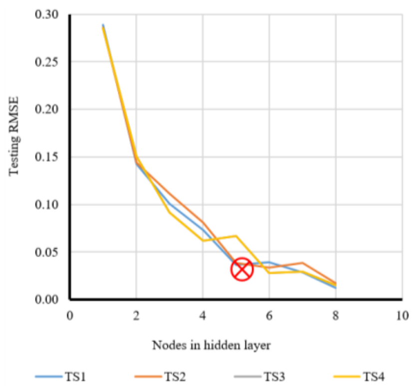


(d)

Fig. 11 Sensitivity analysis of the $R^2$ and RMSE of various suggested MLP predict $P_{ult}$

(23) (see Fig. 10(a))

$$c_i^t = Antlion_j^t + c^t \tag{7}$$

$$d_i^t = Antlion_j^t + d^t \tag{8}$$

The fitness of the prey is contributed to the hunting capability of the ant lions. This is because it is supposed that each hunter hunts one prey. A so-called function "roulette wheel selection (RWS)" is applied for this purpose. The victim sliding in the trap (see Fig. 10(b)) is mathematically modeled by Eqs. (24) and (25).

$$c^t = c^t / I \tag{9}$$

$$d^t = d^t / I \tag{10}$$

where $I$ represent a factor that depends on the ratio of the flowing iteration and the number of iterations, notably, this decrease in space results in a better convergence in the optimization process.

Eventually, updating the position of the members and catching the prey are expressed as follows

$$f(Ant_i^t) < f\left(Antlion_j^t\right) \rightarrow Antlion_j^t = Ant_i^t \tag{11}$$

After determining the best search agent, its position is considered to influence the position of other members. To define this

$$Ant_i^t = {R_A^t + R_E^t}/{2} \tag{12}$$

in which $R_A^t$ is a random walk of the prey near the hunter selected through the RWS, and $R_E^t$ denotes the random walk of that prey near the best ant lion (Mirjalili 2015).

## 3. Results and discussion

### 3.1 MLP Optimization process

The effectiveness of several multilayer perceptron-based networks was assessed in this section. In a multilayer perceptron-based networks model, the neurons number for the output and also input layers are continuously taken. Such a number is typically considered to be equal to the number of output and inputs, respectively. It is essential to know that the neurons number in the hidden layer is a different factor that changes relying on the amount of user data. So, in this step and to create a strong multilayer perceptron-based networks structure eight different systems were taken into consideration. Also, for more trustworthiness, the calculation of each of the proposed multilayer perceptron-based networks was repeated six times, and totally, forty-eight various structures were built to specify the most proper structure. Fig. 11 shows the results of considered analysis (i.e., respectively for the $R^2$ and RMSE, respectively). This trial and error procedure can help to determine the most structure of the optimized network. As seen, to predict the $P_{ult}$ of the considered footing, the best arrangement of the MLP model with having the smallest error may be achieved while the neurons number in each hidden layer is identical to 5. Accordingly, to have a simplified solution and as shown in Fig. 11, the number of nodes equal to five was selected as the best possible neuron number that requires to be chosen in the hidden layers. This will help to find a strong multilayer perceptron-based network structure, which in this section obtained to be 4×5×1 (i.e., four input layers, five neurons in a single hidden layer, and one output layer which is $P_{ult}$). It should be noted that in the last part of the present work, various reduced formulas are specified according to changes done on the nodes number in a single hidden layer.

### 3.2 The proposed Hybrid model combined with MLP in the prediction of $\boldsymbol{P_{ult}}$

Similar to the optimization method that was used for the MLP technique, a trial and error process was employed with the target of a hybrid dragonfly algorithm (DA), whale optimization algorithm (WOA), and ant lion optimization (ALO). To specify a suitable structure, various population sizes are chosen in performing the DA-MLP, WOA-MLP, and ALO-MLP algorithms. The results of this section are explained using means of the RMSE performance network reduction path. Several sizes of the population are taken (i.e., between 25 to 500, as shown in Figs. 12(a) and (b)). In

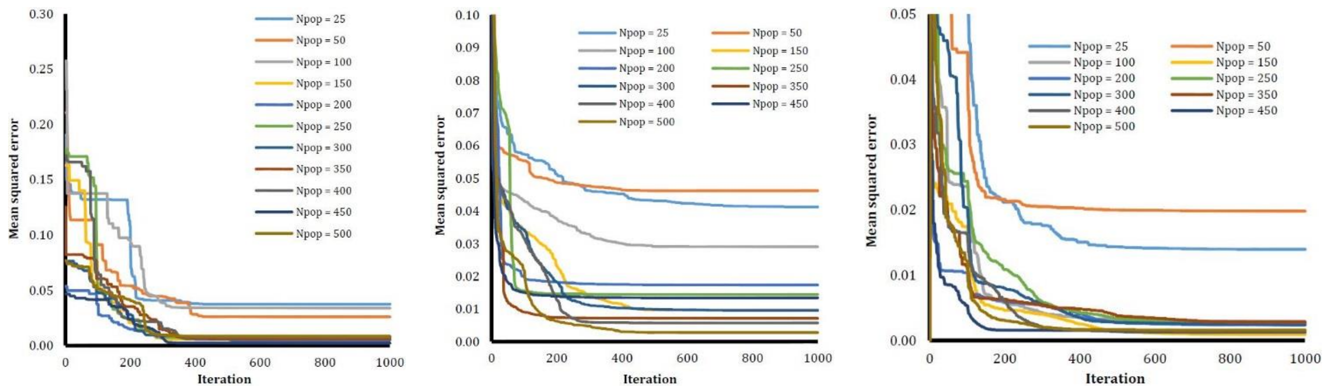


(a) DA-MLP (b) WOA-MLP (c) ALO-MLP

Fig. 12 Efficiency results for various population size values in the estimation of (a) DA-MLP; (b) WOA-ML; (c) ALO-MLP

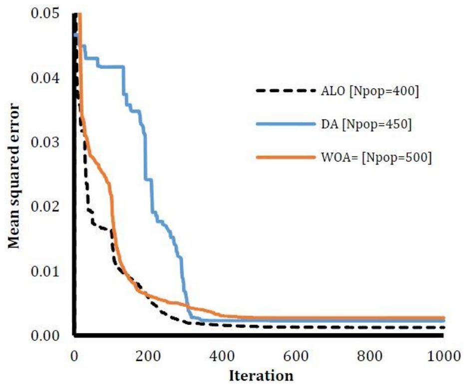


Fig. 13 The minimum MSE outputs of proposed models

this regard and after all trial and error progress, the proposed DA-MLP network performance (i.e., after 1000 iterations) is shown in Fig. 12(a). As in the optimized DA-MLP structure, the minimum MSE obtained when the population is equal to 250. The minimum MSE outputs of the proposed models are compared and shown in Fig. 13. Results of training and testing for different proposed DA-MLP, WOA-MLP, and ALO-MLP models are tabulated in Tables 2, 3, and 4, respectively. It can be seen that in the DA-MLP, WOA-MLP, and ALO-MLP proposed techniques, the most accurate predictive networks can be found if the population size set to be 450, 500, and 400, respectively. In this regard, the $R^2$ and RMSE of (0.996 and 0.046) and (0.995 and 0.088) were found for the training and testing datasets of the DA-MLP technique. Similarly, the $R^2$ and RMSE of (0.996 and 0.051) and (0.985 and 0.053) were found for the training and testing datasets of the WOA-MLP proposed predictive network. Besides, the $R^2$ and RMSE of (0.998 and 0.034) and (0.998 and 0.053) were found for the training and testing datasets of ALO-MLP proposed predictive network. Noting that both of the above networks have received rank number one regarding the accuracy of the precision when compared to the measured uplift force in the laboratory. Population-based sensitivity analysis of DA-

Table 2 Results of training and testing for different proposed DA-MLP models

| Population size | Network result | | | | Ranking | | | | **Total rank** | **RANK** |
|---|---|---|---|---|---|---|---|---|---|---|
| | Train | | Test | | Train | | Test | | | |
| | $R^2$ | RMSE | $R^2$ | RMSE | $R^2$ | RMSE | $R^2$ | RMSE | | |
| 25 | 0.937 | 0.186 | 0.918 | 0.216 | 1 | 1 | 1 | 2 | **5** | 11 |
| 50 | 0.941 | 0.155 | 0.938 | 0.283 | 2 | 3 | 3 | 1 | **9** | 10 |
| 100 | 0.956 | 0.177 | 0.923 | 0.200 | 3 | 2 | 2 | 3 | **10** | 9 |
| 150 | 0.991 | 0.071 | 0.985 | 0.090 | 9 | 9 | 7 | 9 | **34** | 3 |
| 200 | 0.993 | 0.067 | 0.982 | 0.099 | 10 | 10 | 5 | 8 | **33** | 4 |
| 250 | 0.989 | 0.075 | 0.979 | 0.107 | 7 | 7 | 4 | 7 | **25** | 6 |
| 300 | 0.983 | 0.089 | 0.985 | 0.175 | 5 | 4 | 6 | 4 | **19** | 8 |
| 350 | 0.989 | 0.074 | 0.991 | 0.143 | 6 | 8 | 8 | 6 | **28** | 5 |
| 400 | 0.990 | 0.084 | 0.998 | 0.072 | 8 | 6 | 11 | 11 | **36** | 2 |
| 450 | 0.996 | 0.046 | 0.995 | 0.088 | 11 | 11 | 9 | 10 | **41** | 1 |
| 500 | 0.983 | 0.088 | 0.996 | 0.172 | 4 | 5 | 10 | 5 | **24** | 7 |

Table 3 Results of training and testing for different proposed WOA-MLP models

| Population size | Network result | | | | Ranking | | | | **Total rank** | **RANK** |
|---|---|---|---|---|---|---|---|---|---|---|
| | Train | | Test | | Train | | Test | | | |
| | $R^2$ | RMSE | $R^2$ | RMSE | $R^2$ | RMSE | $R^2$ | RMSE | | |
| 25 | 0.933 | 0.195 | 0.908 | 0.228 | 2 | 2 | 2 | 2 | **8** | 10 |
| 50 | 0.920 | 0.207 | 0.842 | 0.304 | 1 | 1 | 1 | 1 | **4** | 11 |
| 100 | 0.963 | 0.164 | 0.967 | 0.176 | 3 | 3 | 4 | 3 | **13** | 9 |
| 150 | 0.985 | 0.095 | 0.988 | 0.092 | 8 | 7 | 11 | 9 | **35** | 2 |
| 200 | 0.976 | 0.127 | 0.959 | 0.143 | 4 | 4 | 3 | 6 | **17** | 8 |
| 250 | 0.979 | 0.116 | 0.970 | 0.123 | 5 | 5 | 5 | 7 | **22** | 7 |
| 300 | 0.984 | 0.094 | 0.971 | 0.158 | 7 | 8 | 6 | 4 | **25** | 6 |
| 350 | 0.989 | 0.081 | 0.985 | 0.094 | 10 | 9 | 8 | 8 | **35** | 2 |
| 400 | 0.986 | 0.073 | 0.981 | 0.149 | 9 | 10 | 7 | 5 | **31** | 5 |
| 450 | 0.984 | 0.111 | 0.987 | 0.051 | 6 | 6 | 10 | 11 | **33** | 4 |
| 500 | 0.996 | 0.051 | 0.985 | 0.053 | 11 | 11 | 9 | 10 | **41** | 1 |

Table 4 Results of training and testing for different proposed ALO-MLP models

| Population size | Network result | | | | Ranking | | | | **Total rank** | **RANK** |
|---|---|---|---|---|---|---|---|---|---|---|
| | Train | | Test | | Train | | Test | | | |
| | $R^2$ | RMSE | $R^2$ | RMSE | $R^2$ | RMSE | $R^2$ | RMSE | | |
| 25 | 0.979 | 0.114 | 0.940 | 0.185 | 2 | 2 | 1 | 2 | **7** | 11 |
| 50 | 0.976 | 0.135 | 0.982 | 0.099 | 1 | 1 | 2 | 5 | **9** | 10 |
| 100 | 0.994 | 0.052 | 0.988 | 0.115 | 5 | 3 | 4 | 3 | **15** | 9 |
| 150 | 0.998 | 0.029 | 0.992 | 0.100 | 9 | 11 | 7 | 4 | **31** | 3 |
| 200 | 0.991 | 0.047 | 0.990 | 0.265 | 3 | 7 | 5 | 1 | **16** | 8 |
| 250 | 0.996 | 0.051 | 0.993 | 0.068 | 8 | 5 | 8 | 8 | **29** | 4 |
| 300 | 0.994 | 0.048 | 0.990 | 0.096 | 6 | 6 | 6 | 6 | **24** | 6 |
| 350 | 0.994 | 0.051 | 0.996 | 0.076 | 4 | 4 | 9 | 7 | **24** | 6 |
| 400 | 0.998 | 0.034 | 0.998 | 0.053 | 11 | 10 | 11 | 9 | **41** | 1 |
| 450 | 0.995 | 0.038 | 0.987 | 0.038 | 7 | 9 | 3 | 10 | **29** | 4 |
| 500 | 0.998 | 0.038 | 0.997 | 0.038 | 10 | 8 | 10 | 11 | **39** | 2 |

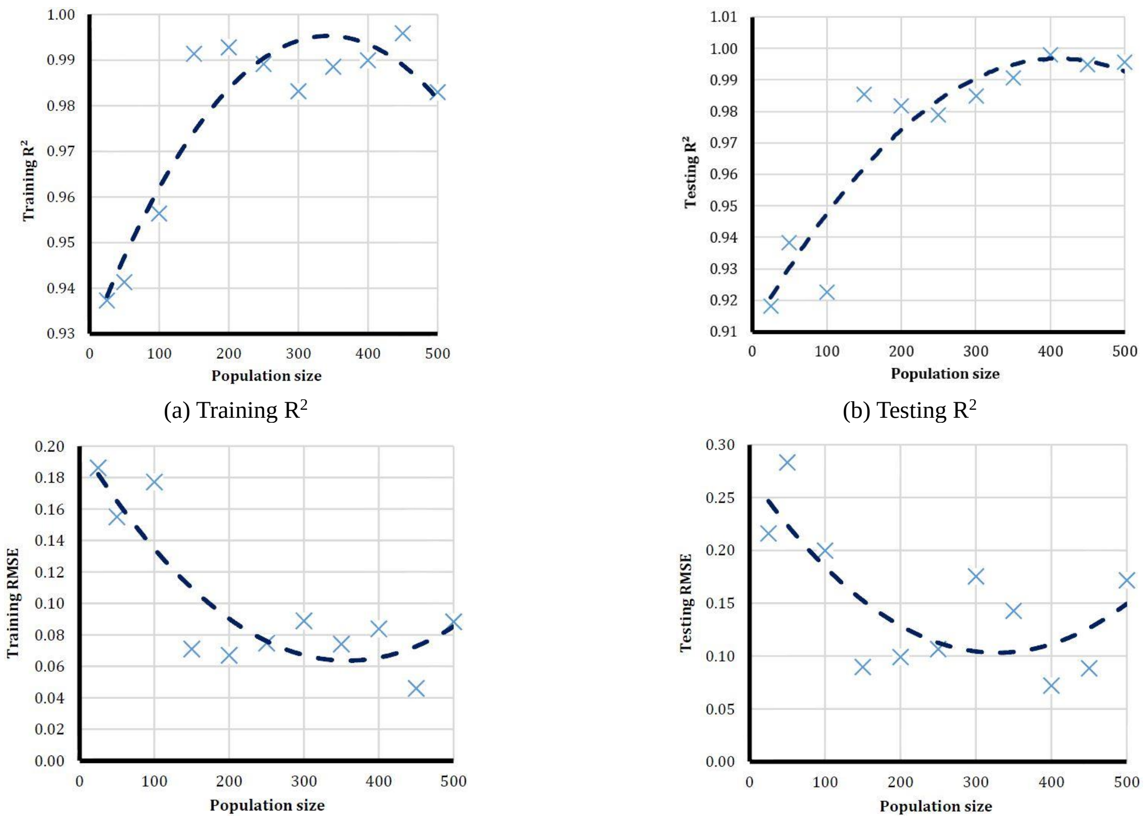


(a) Training $R^2$ (b) Testing $R^2$

(c) Training RMSE (d) Training RMSE

Fig. 14 Population-based Sensitivity analysis of DA-MLP: (a) Training $R^2$; (b) Testing $R^2$; (c) Training RMSE; (d) Training RMSE

MLP, WOA-MLP, and ALO-MLP for both of the training and testing, considering the $R^2$ and RMSE statistical indices, are shown in Figs. 14-16, respectively.

### *3.3 Model assessment and future direction*

This part presents the accuracy results of three developed structures for the prediction of the $P_{ult}$. Several attempts have been performed to illustrates the importance of the proper selection of neurons number for each hidden layer. Fig. 17 showing the details of the comparison between real values that are obtained from the small-scale laboratory study and the one we received from proposed predictive networks. The high level of accuracy in the prediction of $P_{ult}$ shows that models can be successful in predicting such a complex problem. In this regard, the

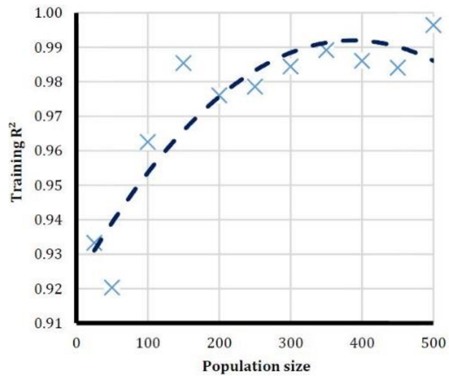


(a) Training $R^2$

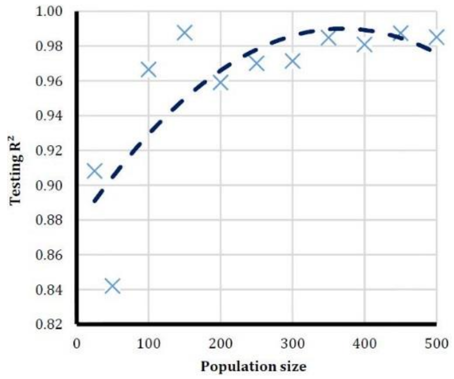


(b) Testing $R^2$

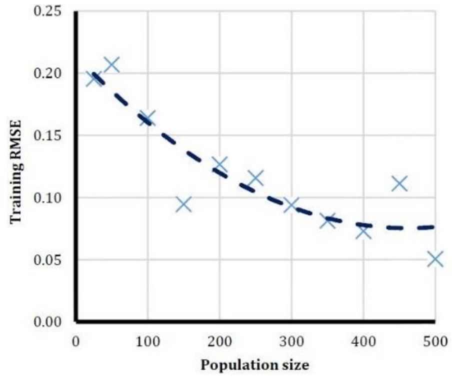


(c) Training RMSE

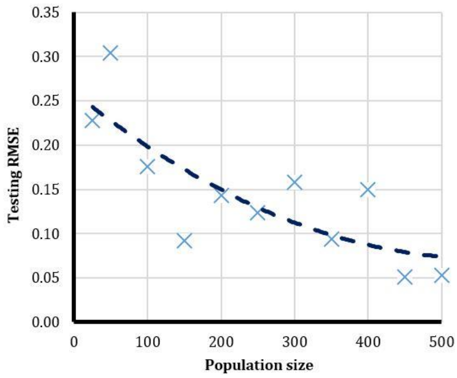


(d) Training RMSE

Fig. 15 Population-based Sensitivity analysis of WOA-MLP: (a) Training $R^2$; (b) Testing $R^2$; (c) Training RMSE; (d) Training RMSE

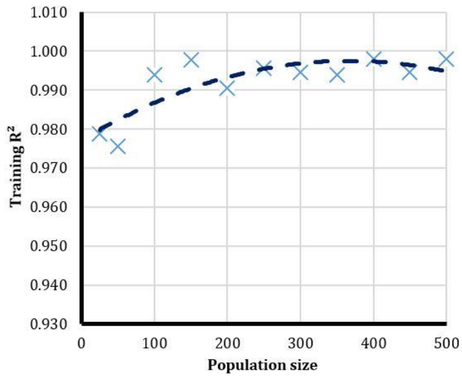


(a) Training $R^2$

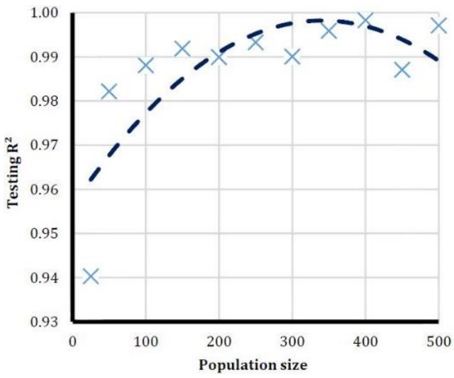


(b) Testing $R^2$

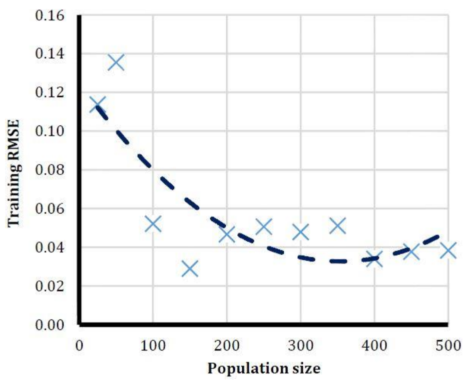


(c) Training RMSE

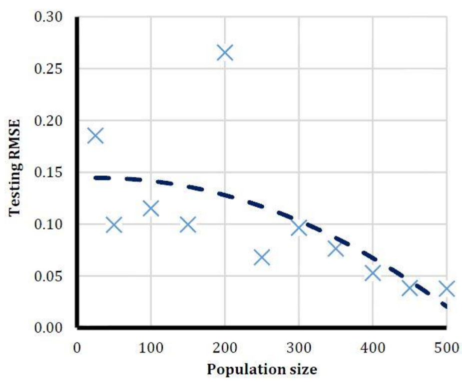


(d) Training RMSE

Fig. 16 Population-based Sensitivity analysis of ALO-MLP: (a) Training $R^2$; (b) Testing $R^2$; (c) Training RMSE; (d) Training RMSE

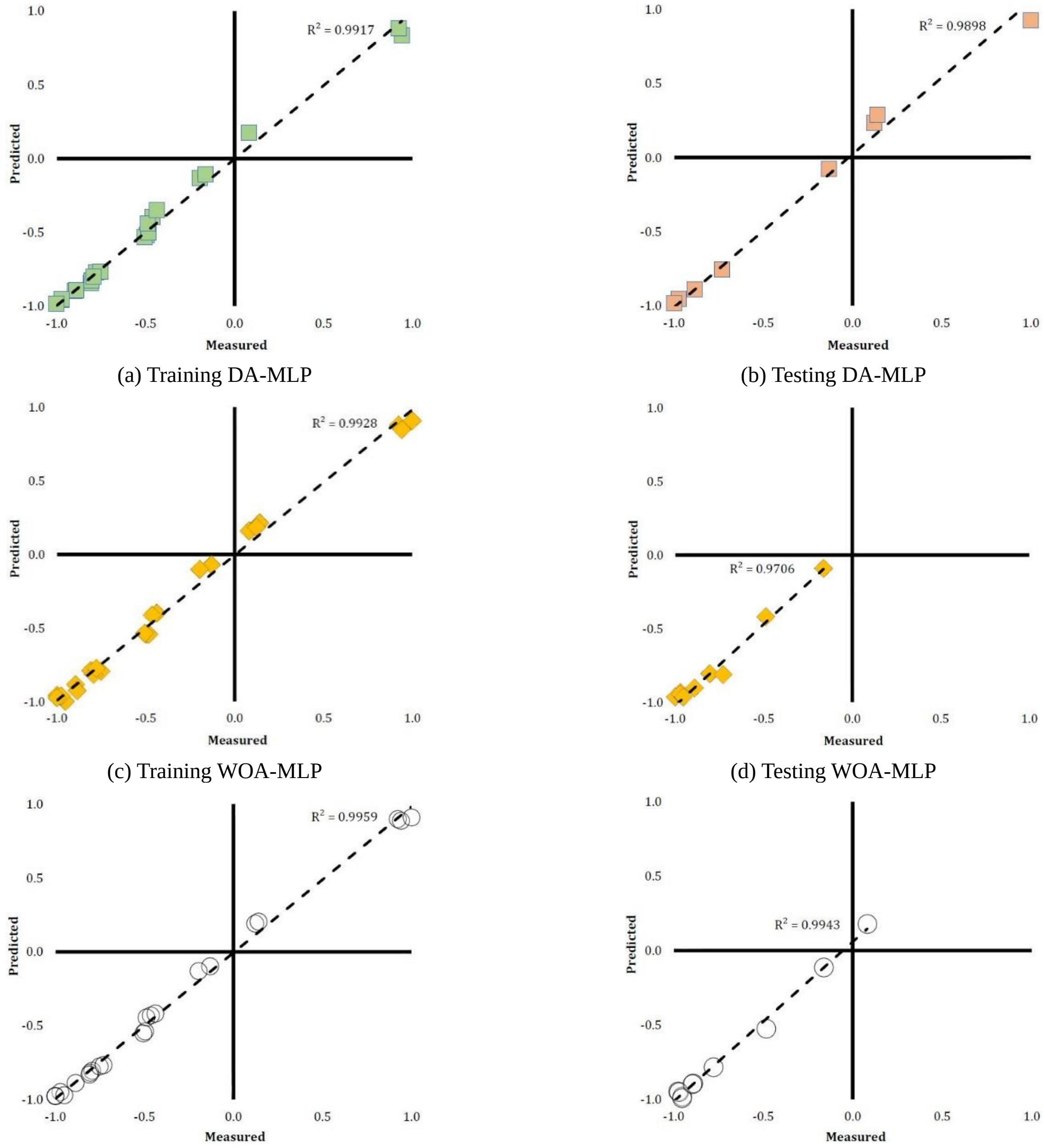


(a) Training DA-MLP (b) Testing DA-MLP

(c) Training WOA-MLP (d) Testing WOA-MLP

(e) Training ALO-MLP (f) Training ALO-MLP

Fig. 17 The performance results of the final: (a) Training DA-MLP; (b) Testing DA-MLP; (c) Training WOA-MLP; and (d) Training WOA-MLP; (E) Training WOA-MLP; and (F) Training WOA-MLP

performance results of the final proposed methods, namely (a) optimized DA-MLP (Figs. 17(a)-(b)); (b) WOA-MLP (Figs. 17(c)-(d)); and (c) ALO-MLP (Figs. 17(e)-(f)). The results of the ultimate pullout capacity obtained from the enlarged piles, as well as those outputs we received from three nominated hybrid models, are compared together in Fig. 17. In this sense, Fig. 18(a) shows the time taken for running fourteen different techniques showing the proposed technique are reasonable acceptable in regard to the calculation time (Fig. 18(a)). Fig. 18(b) illustrated the time taken to perform the population-based sensitivity analysis for the three proposed algorithms namely, DA-MLP, WOA-MLP, and ALO-MLP. The time outputs reveal the DA-MLP is the slowest algorithm where the WOA-MLP found to be the fastest technique.

Table 5 evaluated the final output of best-fit proposed hybridized predictive networks (e.g., WOA-MLP, ALO-MLP, DA-MLP). It can be seen that for the proposed DA-MLP (i.e., the swarm size equal to 450), WOA-MLP (i.e., the swarm size similar to 500), and ALO-MLP (i.e., the swarm size equal to 400), the total score obtained to be 10, 9, and 4 (i.e., out of 12), respectively. The results obtained from Table 5 show that the DA-MLP can be proposed as the best-fit hybrid mathematical solutions among the proposed methods due to a total score of 10 out of 12.

## 4. Conclusions

In the current study, the main target was to understand

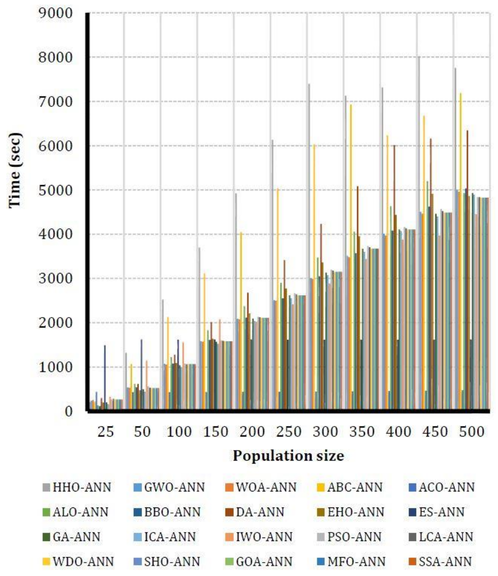


(a)

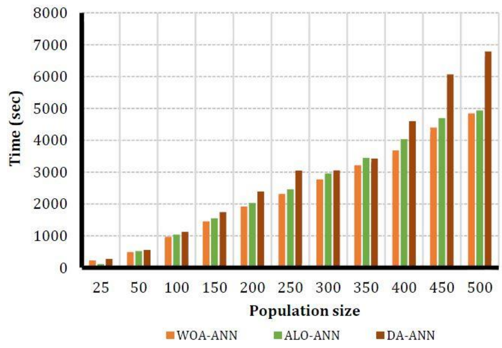


(b)

Fig. 18 Time is taken to perform the population-based sensitivity analysis for the three proposed algorithms

Table 5 Scoring the best-fit hybridized structures

| Best fit | Swarm size | Training network | | Testing network | | | | | | Total score |
|---|---|---|---|---|---|---|---|---|---|---|
| | | $R^2$ | RMSE | $R^2$ | RMSE | $R^2$ | RMSE | $R^2$ | RMSE | |
| DA-MLP | 450 | 0.9917 | 0.0460 | 0.9898 | 0.0880 | 3 | 2 | 2 | 3 | 10 |
| WOA-MLP | 500 | 0.9928 | 0.0510 | 0.9706 | 0.0530 | 2 | 3 | 3 | 1 | 9 |
| ALO-MLP | 400 | 0.9959 | 0.0340 | 0.9943 | 0.0530 | 1 | 1 | 1 | 1 | 4 |

the importance of population sensitivity analysis of two-hybrid mathematical solutions. Such analysis will help us to understand the proper structure of a trustworthy predictive approach. To do so, 36 examples of small-scale load-settlement of laboratory experiments of under reamed piles (embedded in a cohesionless environment) are performed. Accordingly, the ultimate uplift capacity of such piles ($p_{ult}$). After presenting the three applied solutions in this study, namely multilayer perceptron and hybrid DA-MLP, WOA-MLP, and ALO-MLP, are implemented. The results proved that suggested approaches have satisfactory prediction outcomes in predicting $P_{ult}$. However, with the help of population sensitivity analysis, the optimized ALO-MLP model provided better accuracy for the predictive network. Noting that both of the proposed hybrid techniques showed far better accuracy than the conventional model of MLP in the estimation of $P_{ult}$. The learning approach is proper in all three predictive models. In the optimal DA-MLP, WOA-MLP, and ALO-MLP predictive approaches, the $R^2$ for the testing databases were 0.995, 0.985, and 0.998, respectively. Similarly, for the proper structure of DA-MLP, WOA-MLP, and ALO-MLP, the RMSE of the testing datasets were 0.088, 0.053, and 0.053, respectively. The feasibility of ALO-MLP and WOA-MLP to predict the $P_{ult}$ is promising. However, after swarm population-based considerations, the results prove the superiority of the proposed ALO-MLP structure.

## References


Alavi, A.H., Aminian, P., Gandomi, A.H. and Esmaeili, M.A. (2011), "Genetic-based modeling of uplift capacity of suction caissons", *Expert Syst. Applicat.*, **38**(10), 12608-12618. https://doi.org/10.1016/j.eswa.2011.04.049

Ardalan, H., Eslami, A. and Nariman-Zadeh, N. (2009), "Piles shaft capacity from CPT and CPTu data by polynomial neural networks and genetic algorithms", *Comput. Geotech.*, **36**(4), 616-625. https://doi.org/10.1016/j.compgeo.2008.09.003

Bozorgvar, M. and Zahrai, S.M. (2019), "Semi-active seismic control of a 9-story benchmark building using adaptive neural-fuzzy inference system and fuzzy cooperative coevolution", *Smart Struct. Syst., Int. J.*, **23**(1), 1-14. https://doi.org/10.12989/sss.2019.23.1.001

Bui, D.T., Moayedi, H., Gör, M., Jaafari, A. and Foong, L.K. (2019a), "Predicting slope stability failure through machine learning paradigms", *ISPRS Int. J. Geo-Inform.*, **8**(9), 395. https://doi.org/10.3390/ijgi8090395

Bui, D.T., Moayedi, H., Mu'azu, M.A., Rashid, A.S.A. and Nguyen, H. (2019b), "Prediction of pullout behaviour of belled piles thorough various machine learning modelling techniques", *Sensors*, **19**(17), 3678. https://doi.org/10.3390/s19173678

Chae, D., Cho, W. and Na, H.Y. (2012), "Uplift capacity of belled pile in weathered sandstones", *Int. J. Offshore Polar Eng.*, **22**(4), 297-305.

Chen, H., Zhang, Q., Luo, J., Xu, Y. and Zhang, X. (2020), "An enhanced Bacterial Foraging Optimization and its application for training kernel extreme learning machine", *Appl. Soft Comput.*, **86**, 105884. https://doi.org/10.1016/j.asoc.2019.105884

Cheng, M.-Y., Cao, M.-T. and Tran, D.-H. (2014), "A hybrid fuzzy inference model based on RBFNN and artificial bee colony for predicting the uplift capacity of suction caissons", *Automat. Constr.*, **41**, 60-69. https://doi.org/10.1016/j.autcon.2014.02.008

Duan, Y.F., Chen, Q.Y., Zhang, H.M., Yun, C.B., Wu, S.K. and Zhu, Q. (2019), "CNN-based damage identification method of tied-arch bridge using spatial-spectral information", *Smart Struct. Syst., Int. J.*, **23**(5), 507-520. https://doi.org/10.12989/sss.2019.23.5.507

El-Bakry, M.Y. (2003), "Feed forward neural networks modeling for K–P interactions", *Chaos Solitons Fractals*, **18**(5), 995-1000. https://doi.org/10.1016/S0960-0779(03)00068-7

Ghiasi, R. and Ghasemi, M.R. (2018), "Optimization-based method for structural damage detection with consideration of uncertainties- a comparative study", *Smart Struct. Syst., Int. J.*, **22**(5), 561-574. https://doi.org/10.12989/sss.2018.22.5.561

Guo, Z., Moayedi, H., Foong, L.K. and Bahiraei, M. (2020), "Optimal modification of heating, ventilation, and air conditioning system performances in residential buildings using the integration of metaheuristic optimization and neural computing", *Energy Build.*, **214**, 109866. https://doi.org/10.1016/j.enbuild.2020.109866

Hagan, M.T. and Menhaj, M.B. (1994), "Training feedforward networks with the marquardt algorithm", *IEEE Trans. Neural Netw*., **5**(6), 989-993. https://doi.org/10.1109/72.329697

Hebb, D. (1949), *The Organization of Behavior: A Neurophysiological Approach*, Wiley, [JH].

Hertz, J.A. (2018), *Introduction to the Theory of Neural Computation*, CRC Press.

Hornik, K., Stinchcombe, M. and White, H. (1989), "Multilayer feedforward networks are universal approximators", *Neural Networks*, **2**(5), 359-366.

Jain, A.K., Mao, J. and Mohiuddin, K.M. (1996), "Artificial neural networks: A tutorial", *Computer*, **29**(3), 31-44. https://doi.org/10.1109/2.485891

Li, A., Fang, Q., Zhang, D.L., Luo, J.W. and Hong, X.F. (2018), "Blast vibration of a large-span high-speed railway tunnel based on microseismic monitoring", *Smart Struct. Syst., Int. J.*, **21**(5), 561-569. https://doi.org/10.12989/sss.2018.21.5.561

McCulloch, W.S. and Pitts, W. (1943), "A logical calculus of the ideas immanent in nervous activity", *Bull. Mathe. Biophys.*, **5**(4), 115-133. https://doi.org/10.1007/BF02478259

Mehrabi, M., Pradhan, B., Moayedi, H. and Alamri, A. (2020), "Optimizing an Adaptive Neuro-Fuzzy Inference System for Spatial Prediction of Landslide Susceptibility Using Four State-of-the-art Metaheuristic Techniques", *Sensors*, **20**(6), 1723. https://doi.org/10.3390/s20061723

Mirjalili, S. (2015), "The ant lion optimizer", *Adv. Eng. Software*, **83**, 80-98. https://doi.org/10.1016/j.advengsoft.2015.01.010

Mirjalili, S. (2016), "Dragonfly algorithm: a new meta-heuristic optimization technique for solving single-objective, discrete, and multi-objective problems", *Neural Comput. Applicat.*, **27**(4), 1053-1073. https://doi.org/10.1007/s00521-015-1920-1

Mirjalili, S. and Lewis, A. (2016), "The whale optimization algorithm", *Adv. Eng. Software*, **95**, 51-67. https://doi.org/10.1016/j.advengsoft.2016.01.008

Moayedi, H., Moatamediyan, A., Nguyen, H., Bui, X.-N., Bui, D.T. and Rashid, A.S.A. (2019), "Prediction of ultimate bearing capacity through various novel evolutionary and neural network models", *Eng. Comput.*, **35**. https://doi.org/10.1007/s00366-019-00723-2

Nazir, R., Moayedi, H., Pratikso, A. and Mosallanezhad, M. (2015), "The uplift load capacity of an enlarged base pier embedded in dry sand", *Arab. J. Geosci.*, **8**, 7285-7296. https://doi.org/10.1007/s12517-014-1721-3

Nguyen, H., Moayedi, H., Sharifi, A., Amizah, W.J.W. and Safuan, A.R.A. (2019), "Proposing a novel predictive technique using M5Rules-PSO model estimating cooling load in energy-efficient building system", *Eng. Comput.*, **35**, 1-11. https://doi.org/10.1007/s00366-019-00735-y

Palappan, A. and Thangavelu, J. (2018), "A New Meta Heuristic Dragonfly Optimizaion Algorithm for Optimal Reactive Power Dispatch Problem", *Gazi Univ. J. Sci.*, **31**(4), 1107-1121.

Qiao, W. and Yang, Z. (2019), "Forecast the electricity price of U.S. using a wavelet transform-based hybrid model", *Energy*, **193**, 116704. https://doi.org/10.1016/j.energy.2019.116704

Rana, N. and Latiff, M.S.A. (2018), "A cloud-based conceptual framework for multi-objective virtual machine scheduling using whale optimization algorithm", *Int. J. Innov. Comput.*, **8**(3). https://doi.org/10.11113/ijic.v8n3.199

Rao, S.G. (2000), "Artificial neural networks in hydrology. II: Hydrologic applications", *J. Hydrol. Eng.*, **5**(2), 124-137. https://doi.org/10.1061/(ASCE)1084-0699(2000)5:2(124)

Saleem, M.M. and Jo, H. (2019), "Impact force localization for civil infrastructure using augmented Kalman Filter optimization", *Smart Struct. Syst., Int. J.*, **23**(2), 123-139. https://doi.org/10.12989/sss.2019.23.2.123

Shen, L., Chen, H., Yu, Z., Kang, W., Zhang, B., Li, H., Yang, B. and Liu, D. (2016), "Evolving support vector machines using fruit fly optimization for medical data classification", *Knowledge-Based Syst.*, **96**, 61-75. https://doi.org/10.1016/j.knosys.2016.01.002

Shi, F., Liu, C. and Cai, L.B. (1998), *Experimental Research on Bearing Capacity of Belled Piles*, A a Balkema Publishers, Leiden, pp. 165-170.

Soleimani, S., Jiao, P.C., Rajaei, S. and Forsati, R. (2018), "A new approach for prediction of collapse settlement of sandy gravel soils", *Eng. Compute.*, **34**(1), 15-24. https://doi.org/10.1007/s00366-017-0517-y

Thomas, S., Pillai, G.N., Pal, K. and Jagtap, P. (2016), "Prediction of ground motion parameters using randomized ANFIS (RANFIS)", *Appl. Soft Comput.*, **40**, 624-634. https://doi.org/10.1016/j.asoc.2015.12.013

Tien Bui, D., Moayedi, H., Anastasios, D. and Kok Foong, L. (2019), "Predicting heating and cooling loads in energy-efficient buildings using two hybrid intelligent models", *Appl. Sci.*, **9**(17), 3543. https://doi.org/10.3390/app9173543

Vanishree, J. and Ramesh, V. (2018), "Optimization of size and cost of static var compensator using dragonfly algorithm for voltage profile improvement in power transmission systems", *Int. J. Renew. Energy Res. (IJRER)*, **8**(1), 56-66.

Wang, M. and Chen, H. (2020), "Chaotic multi-swarm whale optimizer boosted support vector machine for medical diagnosis", *Appl. Soft Comput.*, **88**, 105946. https://doi.org/10.1016/j.asoc.2019.105946

Wang, M., Chen, H., Yang, B., Zhao, X., Hu, L., Cai, Z., Huang, H. and Tong, C. (2017), "Toward an optimal kernel extreme learning machine using a chaotic moth-flame optimization strategy with applications in medical diagnoses", *Neurocomputing*, **267**, 69-84. https://doi.org/10.1016/j.neucom.2017.04.060

Wang, B., Moayedi, H., Nguyen, H., Foong, L.K. and Rashid, A.S.A. (2019), "Feasibility of a novel predictive technique based on artificial neural network optimized with particle swarm optimization estimating pullout bearing capacity of helical piles", *Eng. Comput.*, **36**, 1-10. https://doi.org/10.1007/s00366-019-00764-7

Wikelski, M., Moskowitz, D., Adelman, J.S., Cochran, J., Wilcove, D.S. and May, M.L. (2006), "Simple rules guide dragonfly migration", *Biol. Lett.*, **2**(3), 325-329. https://doi.org/10.1098/rsbl.2006.0487

Wu, Y.D., Liu, J. and Chen, R. (2015), "An analytical analysis of a single axially-loaded pile using a nonlinear softening model", *Geomech. Eng., Int. J.*, **8**(6), 769-781. https://doi.org/10.12989/gae.2015.8.6.769

Xi, W., Li, G., Moayedi, H. and Nguyen, H. (2019), "A particle-based optimization of artificial neural network for earthquake-induced landslide assessment in Ludian county, China", *Geomat. Natural Hazards Risk*, **10**(1), 1750-1771. https://doi.org/10.1080/19475705.2019.1615005

Xu, X. and Chen, H.-L. (2014), "Adaptive computational chemotaxis based on field in bacterial foraging optimization", *Soft Comput.*, **18**(4), 797-807. https://doi.org/10.1007/s00500-013-1089-4

Xu, Y., Chen, H., Luo, J., Zhang, Q., Jiao, S. and Zhang, X. (2019), "Enhanced Moth-flame optimizer with mutation strategy for global optimization", *Inform. Sci.*, **492**, 181-203. https://doi.org/10.1016/j.ins.2019.04.022

Yao, W.J. and Chen, S.P. (2014), "Elastic-plastic analytical solutions of deformation of uplift belled pile", *Teh. Vjesn.*, **21**(6), 1201-1211.

Yasen, M., Al-Madi, N. and Obeid, N. (2018), "Optimizing Neural Networks using Dragonfly Algorithm for Medical Prediction", *Proceedings of the 8th International Conference on Computer Science and Information Technology (CSIT)*, pp. 71-76.

Yuan, C. and Moayedi, H. (2019), "Evaluation and comparison of the advanced metaheuristic and conventional machine learning methods for prediction of landslide occurrence", *Eng. Comput.*, **36**. https://doi.org/10.1007/s00366-019-00798-x

Zhang, L.H., Wang, Y.W., Ni, Y.Q. and Lai, S.K. (2018), "Online condition assessment of high-speed trains based on Bayesian forecasting approach and time series analysis", *Smart Struct. Syst., Int. J.*, **21**(5), 705-713. https://doi.org/10.12989/sss.2018.21.5.705

Zhao, X., Li, D., Yang, B., Ma, C., Zhu, Y. and Chen, H. (2014), "Feature selection based on improved ant colony optimization for online detection of foreign fiber in cotton", *Appl. Soft Comput.*, **24**, 585-596. https://doi.org/10.1016/j.asoc.2014.07.024

Zhao, X., Zhang, X., Cai, Z., Tian, X., Wang, X., Huang, Y., Chen, H. and Hu, L. (2019), "Chaos enhanced grey wolf optimization wrapped ELM for diagnosis of paraquat-poisoned patients", *Computat. Biol. Chem.*, **78**, 481-490. https://doi.org/10.1016/j.compbiolchem.2018.11.017

Zhou, G., Moayedi, H., Bahiraei, M. and Lyu, Z. (2020a), "Employing artificial bee colony and particle swarm techniques for optimizing a neural network in prediction of heating and cooling loads of residential buildings", *J. Cleaner Product.*, **254**. https://doi.org/10.1016/j.jclepro.2020.120082

Zhou, G., Moayedi, H. and Foong, L.K. (2020b), "Teaching–learning-based metaheuristic scheme for modifying neural computing in appraising energy performance of building", *Eng. Comput.*, **36**. https://doi.org/10.1007/s00366-020-00981-5

*CC*